Transport and Communications Science Journal, Vol. 71, Issue 4 (05/2020), 347-358

Transport and Communications Science Journal

A METHODOLOGY OF RE-GENERATING A REPRESENTATIVE ELEMENT VOLUME OF FRACTURED ROCK MASS

Hong-Lam DANG*, Phi Hong THINH

University of Transport and Communications, No 3 Cau Giay Street, Hanoi, Vietnam

ARTICLE INFO

TYPE: Research Article
Received: 1/2/2020
Revised: 19/3/2020
Accepted: 19/3/2020
Published online: 28/5/2020
https://doi.org/10.25073/tcsj.71.4.4

* *Corresponding author*
Email: dang.hong.lam@utc.edu.vn

Abstract. In simulation of fractured rock mass such as mechanical calculation, hydraulic calculation or coupled hydro-mechanical calculation, the representative element volume of fractured rock mass in the simulating code is very important and give the success of simulation works. The difficulties of how to make a representative element volume are come from the numerous fractures distributed in different orientation, length, location of the actual fracture network. Based on study of fracture characteristics of some fractured sites in the world, the paper presented some main items concerning to the fracture properties. A methodology of re-generating a representative element volume of fractured rock mass by DEAL.II code was presented in this paper. Finally, some applications were introduced to highlight the performance as well as efficiency of this methodology.

Keywords: fractured rock mass, fracture network, representative element volume, REV, DEAL.II.

1. INTRODUCTION

In simulation of fractured rock mass, the re-generation of discrete fracture network (DFN) is challenged in case the numerous fractures are distributed in different orientation, length and location. An example of complicated fractures illustrated in the Fig. 1 in which fractures can be found on the whole range of scales [1-3]. The understanding and modeling of fracture impacts such as strength, deformation, permeability and anisotropy to the mechanical properties of highly disordered material are complicated [4]. A plenty of engineering

applications such as the extraction of hydrocarbons, the production of geothermal energy, the remediation of contaminated groundwater, and the geological disposal of radioactive waste related to the presence of fracture on rock masses [5]. One of the main key issues of fractured rock mass is how to characterize and represent the geometry of fractures in three-dimensional (3D) discontinuity systems based on limited information from field measurements, [6, 7]. Fracture characteristics are usually taken from lower-dimensional observations with parameters of density, trace lengths, orientation, spacing, and frequency. DFN in 2D or 3D can be created stochastically and can be generated by conducting Monte Carlo simulations [8].

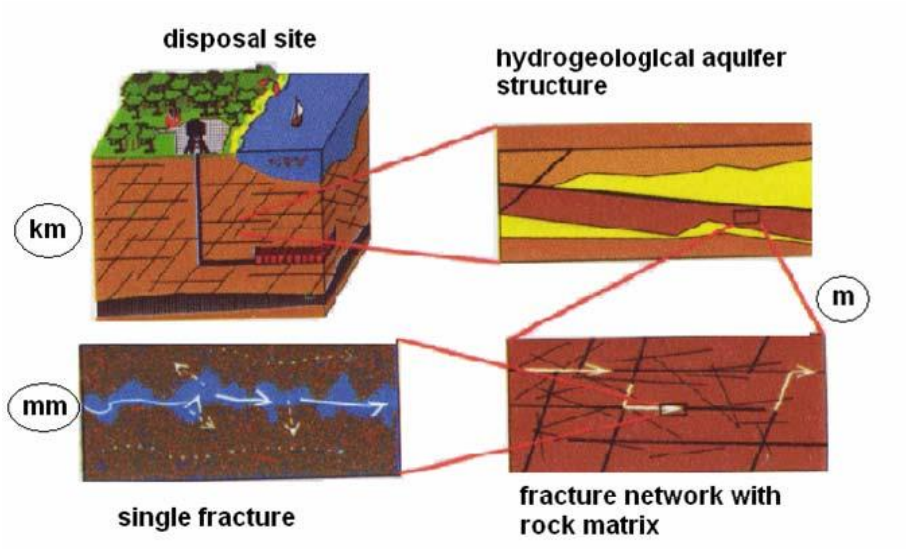

Figure 1. Fractures occur on different scales.

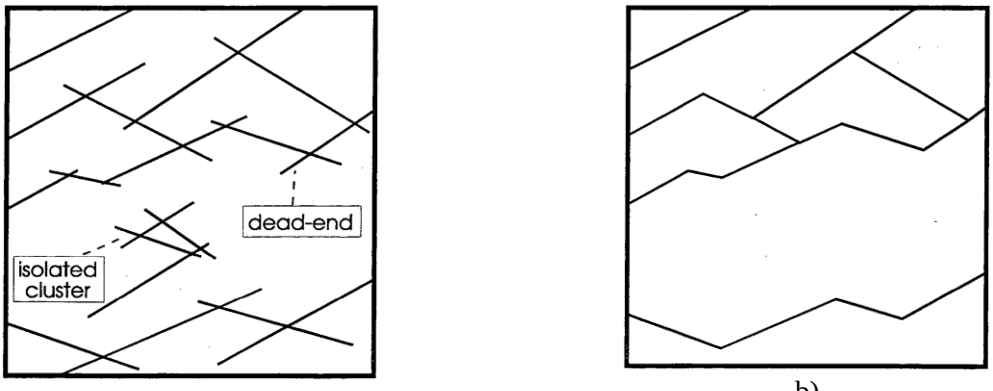

a) b)

Figure 2. sample with dead-end and isolated fractures (a), sample without dead-end and isolated fractures (b).

Generally, natural fracture systems comprise a network of conductive fracture segments, which at both endpoints connect to either the conductive network or to the domain boundary, and a number of non-conductive fracture segments, which connect only at one end-point (see Fig.2). We referred to these non-conductive segments as "dead-ends" [9]. In the simulation works, dead-ends make the more complicated code. That is reason in some cases that dead-ends is ignored [10, 11]. In addition, as mentioned in the literature [10-13], the representative element volume (REV) of fractured rock in many contributions mainly is existed and is

determined. The REV in this paper is prepared for two both cases: sample with dead-ends and sample without dead-ends for varied purposes of further simulations.

The structure of this paper is organized as follows. Following this introduction, the characteristics of fractured rock is outlined. After that, the proposed methodology of re-generation of REV is detailed. The implementation of this methodology in the open source code DEAL.II [14, 15] is used to do for actual Sellafield site [10-13] in order to highlight the performance and efficiency of this methodology. Finally, the paper will be finished with some conclusions.

2. CHARACTERISTICS OF FRACTURED ROCK

In this part, we summarized some main characteristics of fracture network taken from some sites. All necessary data of fractures such as length, orientation, location as well as fractures' aperture will be considered as the input data for the generation of the DFN in the methodology.

2.1. Fracture trace lengths

As studies in literature, a power-law can use to distribute fracture lengths as following equation [10-13]

$$N_F = C.L^{-D} \tag{1}$$

where N_F is the number of fractures per unit area which has fracture length greater than the length L; C is the constant density and D is the fractal dimension.

Number of fracture in a range of fracture length (L_a, L_b) can be taken using Eq. (1) as below:

$$N_F^{ab} = C.\left(L_a^{-D} - L_b^{-D}\right) \tag{2}$$

The parameters C and D are depending on the intensity of fractures.

2.2. Orientations of fractures

The orientations of fractures almost follow a Fisher distribution as the result of some previous studies [10-13]. The probability of the fracture within the direction angle θ is calculated as follow [14]:

$$P(\theta) = \frac{e^{K} - e^{K\cos(\theta)}}{e^{K} - e^{-K}} \tag{3}$$

where K is the Fisher constant for each fracture.

2.3. Location of the fractures

A Poisson distribution has been largely applied for the fracture midpoints [10-13]. The locations of fracture centers are generated by generating random numbers based on a recursive algorithm.

The midpoint coordinates (x_i and y_i) of every fracture through the following equation based on the two coordinate ranges (x_{min}, x_{max}) and (y_{min}, y_{max}) [13]

$$\begin{aligned} x_i &= x_{\min} + R_{x,i}(x_{\max} - x_{\min}) \\ y_i &= y_{\min} + R_{y,i}(y_{\max} - y_{\min}) \end{aligned} \tag{4}$$

where $R_{x,i}$, $R_{y,i}$ are number in the range [0,1]

2.4. Aperture of fractures

In general, the apparent aperture of fracture is the distance between the two surfaces of the fracture. However, depending on the purpose of real applications, it can be the hydraulic aperture which is back-calculated using cubic law equation from laboratory test results of flow rates [16], or it is mechanical aperture for the problem of applied stress acting normal to the mean fracture plane [17]. The fracture aperture can vary by the lognormal distribution as taken from studying the correlation between fracture aperture and trace length [13]. In this study, the initial fracture aperture usually is assumed as being uniform in this study.

3. GENERATION METHODOLOGY OF RE-GENERATING FRACTURE NETWORK

The synthesized data described in the previous part will be used as input for the generation of the fracture network. The methodology to generate DFN realizations is detailed in [18] and which can briefly presented in six steps as below:

Step 0: Input the fractures network's parameters which include the fractal dimensions (*C*, *D*), the Fisher constant (*K*) of different principal sets of fractures and the area of the geometrical model (A).

Step 1: Calculate the number of fractures to be generated for each class of fractures length [l_a , l_b] based on the power law distribution (Eq. 2). The mean value of fracture length of each class is taken as formula l_{ab} = 0.5*(l_a + l_b). The total number of fractures can be evaluated in the model.

Step 2: Determine the number of fracture in each angle interval [θa , θb] by the Fisher distribution corresponding to each principal fracture set (Eq. 3). The mean value of fracture angle taken as formula θab = 0.5*(θa + θb) will be then stored in a list.

Step 3: The list of the center coordinates of all fractures is generated by using the Poisson distribution (Eq. 4)

Step 4: Distribute three parameters (length, angle, and center) for each fracture by followings: with each fracture length lab in step 2, its location and orientation are randomly taken from the list of orientation angle (step 2) and list of center coordinates (step 3). Note that we begin fracture generation from the longest to the shortest fracture. If 20% (*) of fracture length is outside of the domain, the fracture center is suppressed and another center is generated as the above procedure.

Step 5: Adjust fracture length and fracture center. The fracture length and the fracture center will be adjusted in order to keep the difference of total trace length of fractures between the model and the input data less than 5% as Eq. (5)

$$\frac{\left|p_{21}A - L^*\right|}{p_{21}A} \leq 5\% \tag{5}$$

where L^* is the total trace length of fractures in the sample, p_{21} is fracture intensity A is the area of sample. The fracture length will be increased or reduced by factor k in the equation $l^*_{ab} = kl_{ab}$ where k is calculated by Eq. (6)

$$k = \frac{p_{21}A}{L^*} = \frac{p_{21}A}{\sum_1^N l_{ab}} \tag{6}$$

in which l_{ab} is the trace length of fracture before adjustment. The output of DFN (center, length, orientation, total trace length) will be saved in a text file which will be imported in other software for further simulations.

Step 6: Eliminate dead-ends and isolated fractures. All dead-ends of fractures will be deleted first and then all isolated fractures will be ignored. The updated information will be stored in the text file for further simulations.

(*) The proposed value of 20% is tentative value. In reality, the total trace length of all fractures (the p_{21}) may approach the required value if this tentative value (20%) is reduced.

Following the above methodology, the re-generation of representative element volume was implemented in DEAL.II code [14, 15] http://www.dealii.org/. The result of this implementation is showed in following diagram (Fig.3)

4. APPLICATION

In this part, the fractured rock in the Sellafield site is used to re-generate a REV by the above methodology. We chose the Sellafield site for application to this methodology due to plenty of data available in the literature [10-13]

For the Sellafield site, this intensity is not uniform and schematically different zones with density from low to high are distinguished. Correspondingly, the following values are proposed for these two parameters of crack length distribution [10-13]: C is from 1.0 to 4.0 and D is from 2.0 to 2.2 for the Sellafield site. The corresponding fracture intensity p_{20} (defined as the number of fractures per meter square) from 4.8 to 18.3 were determined for this site. Another fracture intensity known as the total trace length per meter square (the parameter p_{21}) was calculated by UoB/NIREX teams University of Birmingham/Nirex (UK) [11] with the corresponding values 4.85 to 16.91 also. The most complicated case for this site (C=4.0 and D=2.2, p_{21}=16.91, p_{20}=18.38) is selected to practice in this paper. There are four principal sets of fracture as resumed in table 1 [10-13].

As in the introduction part, before going to get the fracture distribution, the REV size of fractured rock mass needs to be determined. By studying the REV size be from 0.25m square to 8.0m square for mechanical problem, Min and his colleagues found out the REV exist and its size can be chosen from 2.0m to 6.0m with the coefficient of variation taken from 10% to 5%, respectively [10,11]. Note that the coefficient of variation is defined as the ratio of standard deviation over the mean value [11]. On other hand, in hydraulic problem, the

effective permeability can be taken from 2 m to 8m with the coefficient of variation is 30%, 20% and 10% corresponding to REV of 2m, 5m and 8m, respectively [11]. From above discussions, the smallest size of sample which can be representative for fractured rock of this site is 2m. Hence, an example of the DFN generated for a REV with 2m of size was presented. Firstly, The detailed the number of fractures for each length group and orientation group are listed in the table 2 and 3, respectively for to the case of the high-density crack zone of fracture distributed in the area of the REV (p_{20}=18.38). The total number of fracture is 73 fractures taken from $p_{20}A$. The comparison of fracture distribution for each group respects the theoretical power law distribution showed in figure 4 and 5. Note here that the fractures are generated in the horizontal plane Oxy with the x-axis represents the North direction. The results of step 4 (draft sample), step 5 (sample with dead-end and isolated fractures) and step 6 (sample without dead-end fractures) are illustrated in Figure 6, 7, 8, respectively. The sample at the step 5 gives the fracture intensity p_{20} as the initial value of 18.38 and conformed to the characteristics of fracture distribution such as fracture length, fracture orientation, fracture location as the actual distribution at site.

Table 1. Fracture parameters used for fracture orientation.

Joint Set	Dip/Dip direction (degree)	Fisher constant (K)
1	8/145	5.9
2	88/148	9.0
3	76/21	10.0
4	69/87	10.0

Table 2. Number of fractures distributed in each group of fracture length (result of step 1).

Length arrange		Number
l_a	l_b	
0.5	0.55	14
0.55	0.6	10
0.6	0.65	8
0.65	0.7	6
0.7	0.8	9
0.8	0.9	6
0.9	1	4

Length arrange		Number
l_a	l_b	
1	1.2	5
1.2	1.4	3
1.4	1.6	2
1.6	1.8	1
1.8	2	1
2	2.83 (*)	4
Total		73

(*) 2.83m is the maximum trace length which could be obtained in the REV of 2m size ($2\sqrt{2} = 2.83m$)

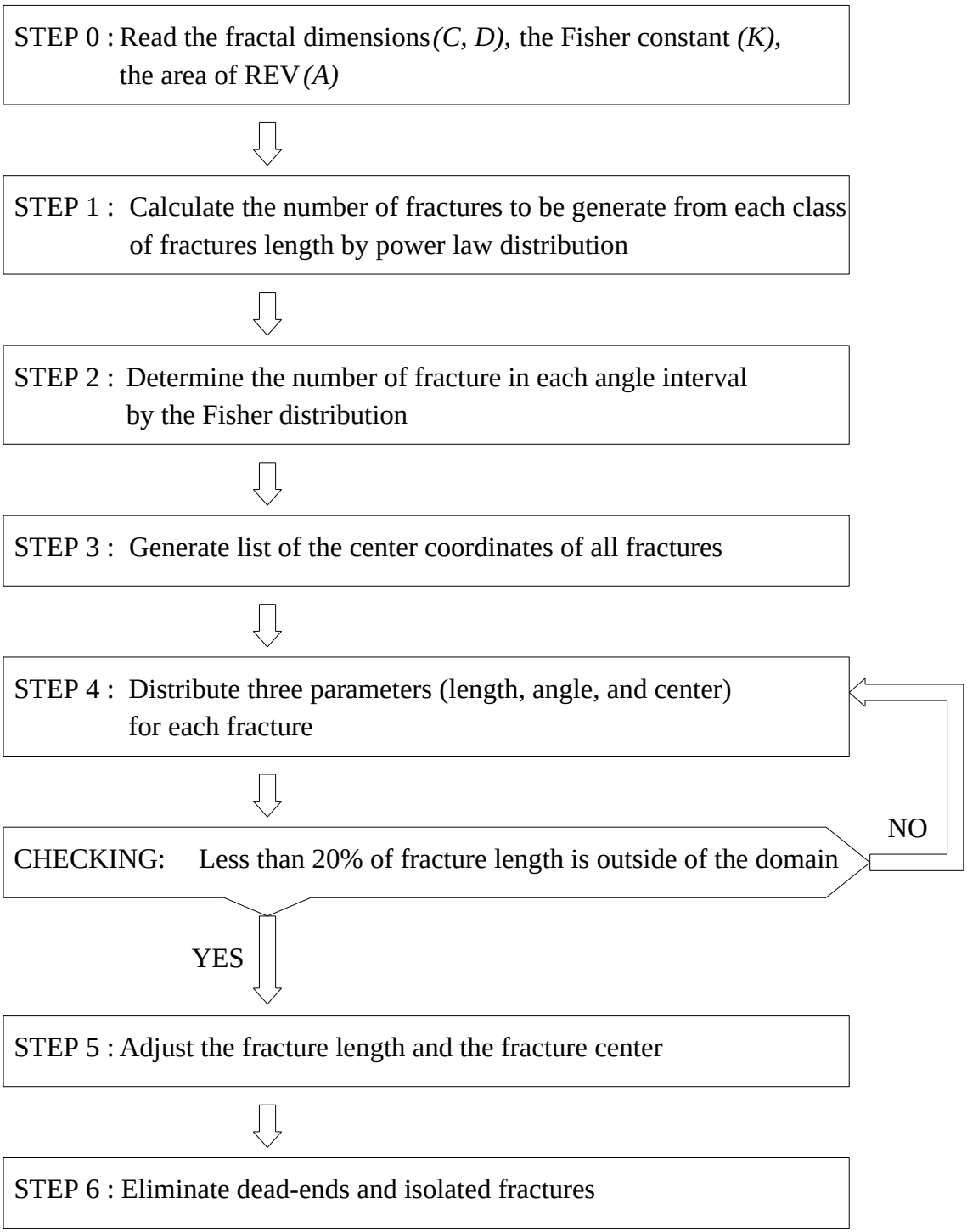

Figure 3. Flow diagram of re-generation code.

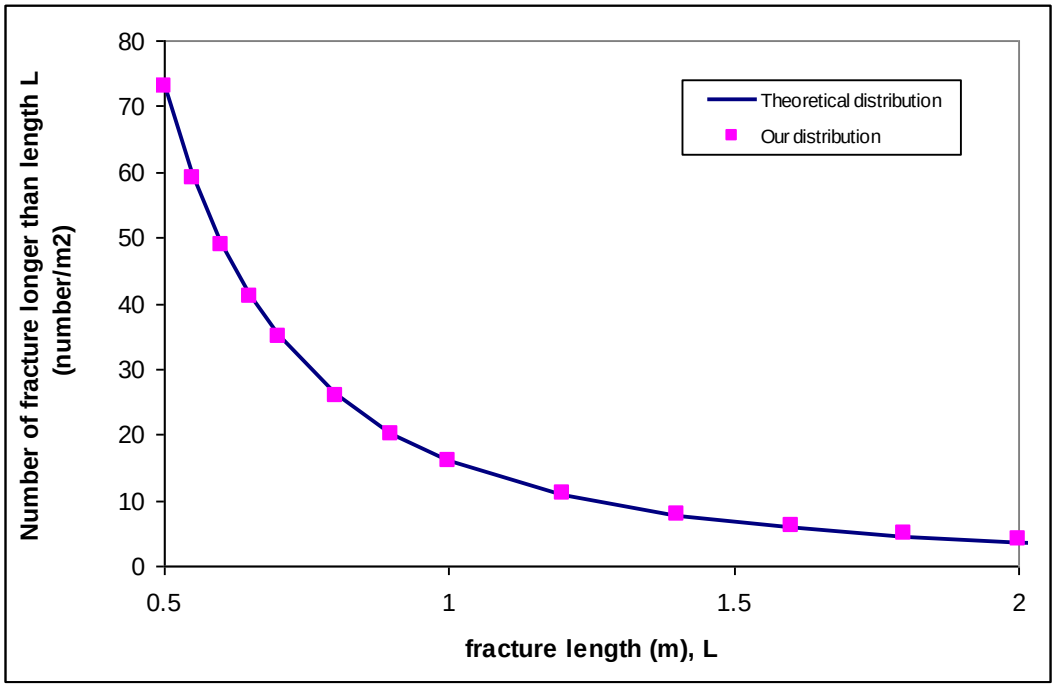

Figure 4. Comparison of fracture number between theoretical distribution and proposed methodology.

Table 3. Fracture number for each fracture set (result of step 2).

Angle to x direction		Fracture number for each fractures set				Total fractures
theta(a)	theta(b)					
-5	5	2	2	3	0	7
5	15	1	1	3	0	5
15	25	1	0	1	0	2
25	35	0	0	2	0	2
35	45	0	0	3	1	4
45	55	0	0	2	1	3
55	65	0	0	1	2	3
65	75	0	0	0	3	3
75	85	0	0	0	2	2
85	95	1	0	0	1	2
95	105	1	1	0	3	5
105	115	2	1	0	3	6
115	125	2	2	0	2	6
125	135	2	3	0	1	6
135	145	1	2	0	0	3
145	155	1	1	0	0	2
155	165	2	2	1	0	5
165	175	2	3	2	0	7
Total		18	18	18	19	73

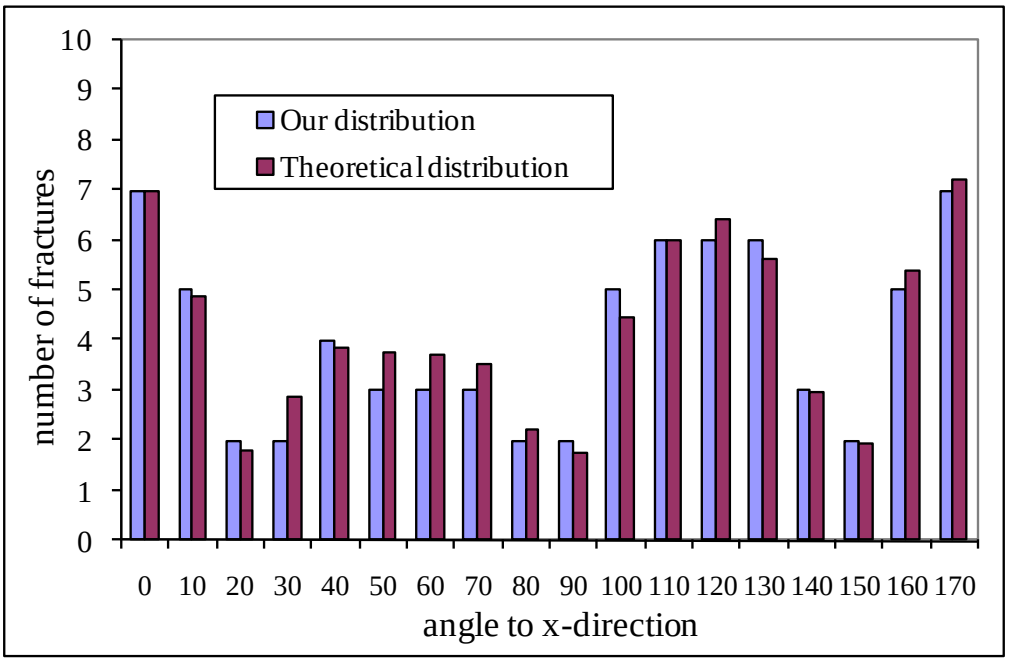

Figure 5. Number of fracture versus the direction angle group.

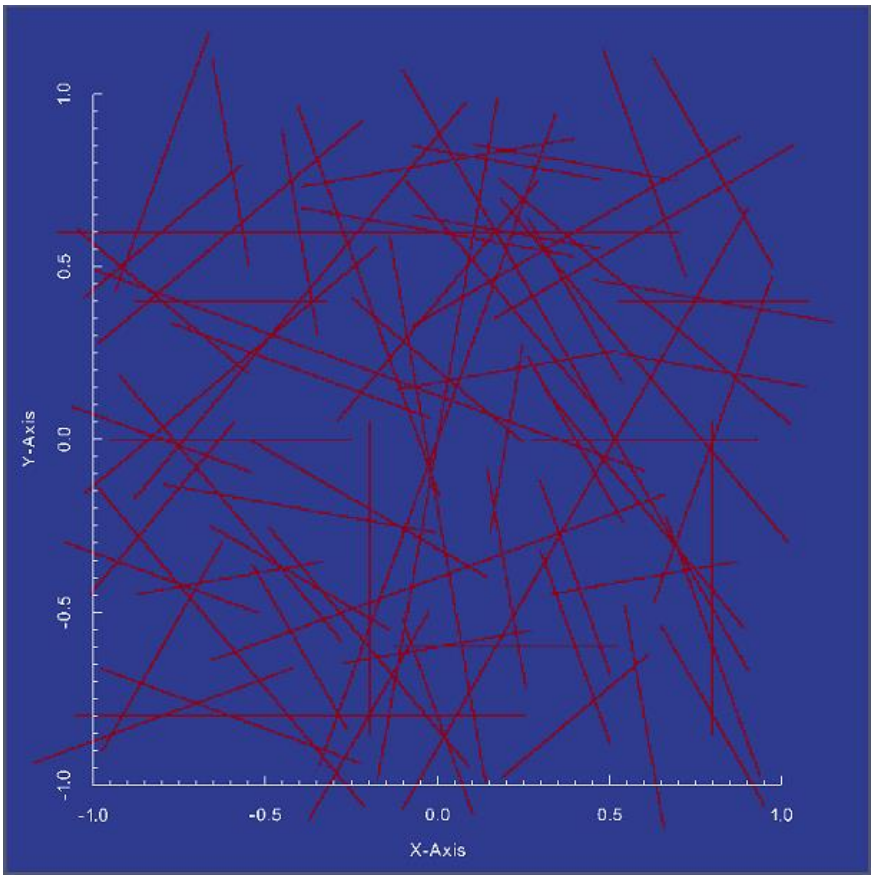

Figure 6. The DFN re-generation process: draft sample (result of step 4).

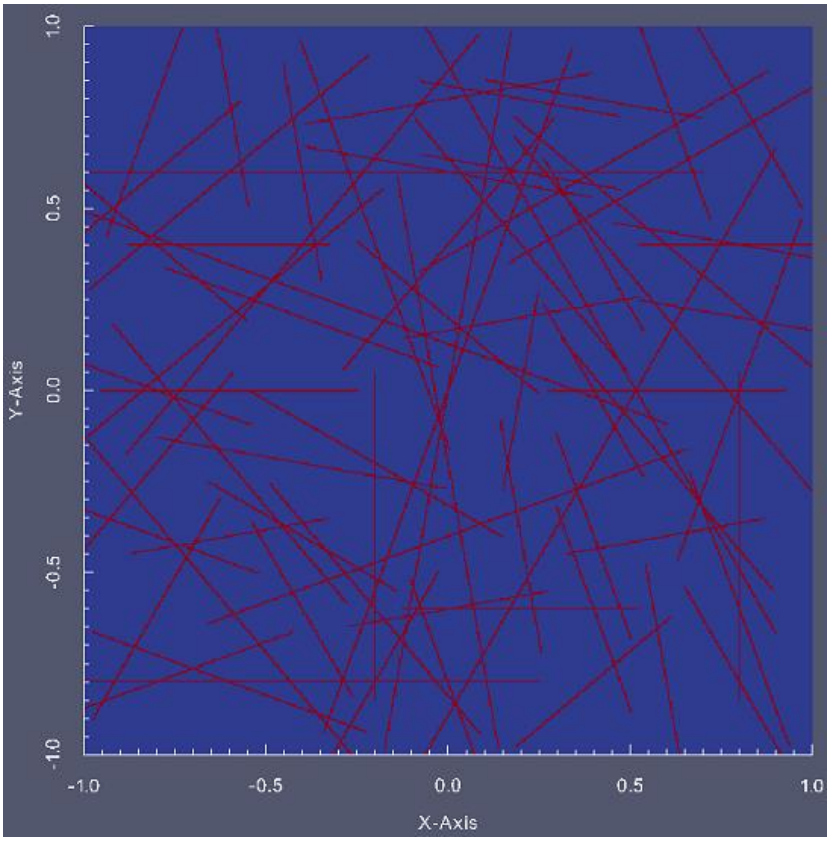

Figure 7. The DFN re-generation process: sample with dead-ends(result of step 5).

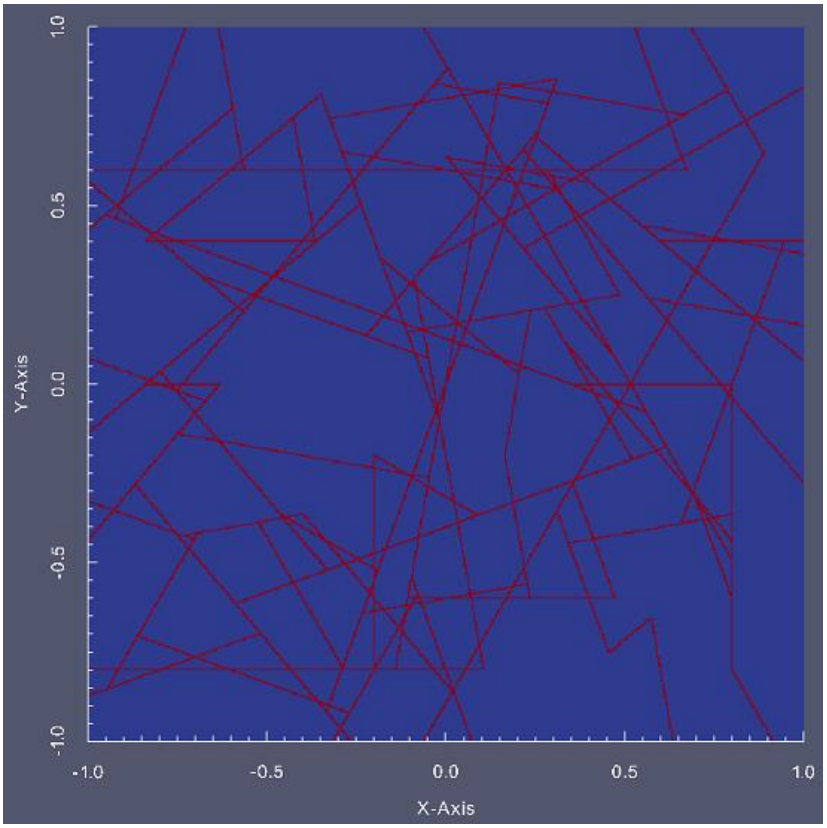

Figure 8. The DFN re-generation process: sample without dead-ends (result of step 6).

5. CONCLUSION

The paper overviews the principle characteristics of fractures in fractured rock mass such as fracture length, fracture orientation, fracture location and fracture aperture of a common site such as the Sellafield site. A methodology of re-generation of a representative element volume of fractured rock mass was proposed and presented. A script code was implemented based on the DEAL library. The efficiency and performance of the proposed methodology is highlighted via an example of Sellafield site in this paper. The result of this methodology can give a material to fur simulation for example: mechanical simulation, hydro-mechanical simulation and cracking propagation, etc…

ACKNOWLEDGEMENTS

This research is funded by University of Transport and Communications (UTC) under grant number T2020-CT-024.

REFERENCES

[1]. Silberhorn-Hemminger, Modeling of fracture aquifer systems: geostatistical analysis and deterministic-stochastic, fracture generation, PhD thesis, Institute for Water and Environmental Systems Modeling, University of Stuttgart, 2002.
[2]. A.-B. Tatomir, Numerical Investigations of Flow through Fractured Porous Media, Master's Thesis, Universität Stuttgart, 2007.
[3]. H.A Nguyen, H.D Nguyen, T.V. Nguyen, X.L Le. Hydraulic Characterization of Fractured Reservoirs: Application on Discrete Fracture Models-Đặc tích hóa thủy động lực của các vỉa chứa nứt nẻ: Ứng dụng mô hình các hệ thống nứt nẻ rời rạc, Journal of Mining and Earth Sciences-Tạp chí KHKT Mỏ - Địa chất), 54, 4/2016, (Chuyên đề Khoan – Khai thác), tr.3-10 (In Vietnamese)
[4]. R. W. Zimmerman, I. Main, Hydromechanical behavior of fractured rocks, in Y. Gueguen, and M. Bouteca (Eds.), Mechanics of Fluid-Saturated Rocks, Elsevier, London, 2004, pp. 363-421.
[5]. J. Rutqvist, O. Stephansson, The role of hydromechanical coupling in fractured rock engineering, Hydrogeol J, 11 (2003) 7–40. https://doi.org/10.1007/s10040-002-0241-5
[6]. Q. Lei, Characterisation and modelling of natural fracture networks: geometry, geomechanics and fluid flow, PhD thesis, Imperial College London, 2016. https://spiral.imperial.ac.uk/handle/10044/1/42358
[7]. W. S Dershowitz, H. H. Einstein, Characterizing rock joint geometry with joint system models, Rock Mech. Rock Eng., 21 (1988) 21–51. https://doi.org/10.1007/BF01019674
[8]. J. C. S. Long, D. M. Billaux, From field data to fracture network modeling: An example incorporating spatial structure. Water Resour. Res., 23 (1987) 1201-1216. https://doi.org/10.1029/WR023i007p01201
[9]. J. Birkholzer, K. Karasaki, FMGN, RENUMN, POLY, TRIPOLY: Suite of Programs for Calculating and Analyzing Flow and Transport in Fracture Networks Embedded in Porous Matrix Blocks, LBNL-39387, 1996. https://digital.library.unt.edu/ark:/67531/metadc685360/
[10].K. B. Min, L. Jing, Numerical determination of the equivalent elastic compliance tensor for fractured rock masses using the distinct element method, Int. J. Rock Mech. Min. Sci., 40 (2003) 795-816. https://doi.org/10.1016/S1365-1609(03)00038-8
[11].K. B. Min, L. Jing, O. Stephansson, Determining the equivalent permeability tensor for fractured rock masses using a stochastic REV approach: Method and application to the field data from Sellafield, UK, Hydrogeo. Jour., 12 (2004) 497–510. https://doi.org/10.1007/s10040-004-0331-7
[12].J. Anderson, I. Staub, L. Knight, Decovalex III/ Benchpar projects, Approaches to Upscaling Thermal-Hydro- Mechanical Processes in a Fractured Rock Mass and its Significance for Large-Scale Repository Performance Assessment, Summary of Findings, Report of BMT2/WP3, 2005. https://inis.iaea.org/search/search.aspx?orig_q=RN:37022239

[13].A. Baghbanan, Scale and Stress Effects on Hydro-Mechanical Properties of Fractured Rock Mass, ISSN 1650-8602, PhD thesis, Royal Institute of Technology, 2008.
[14].Bangerth, G. Kanschat, Concepts for Object-Oriented Finite Element Software— The deal.II Library, Report 99-43, Sonderforschungsbereich 3-59, IWR, Universitat Heidelberg, Heidelberg, Germany, 1999.
[15].W. Bangerth, R. Hartmann and G. Kanschat, Deal.II — a general purpose object oriented finite element library, ACM Trans. Math. Software, 33 (2007). https://doi.org/10.1145/1268776.1268779
[16].S. Ge, A governing equation for fluid flow in rough fractures, Water Resour Res; 33 (1997) 53-61. https://doi.org/10.1029/96WR02588
[17].C.E. Renshaw, J.C. Park, Effect of mechanical interactions on the scaling of fracture length and aperture, Nature 386 (1997) 482–484. https://doi.org/10.1038/386482a0
[18].H.L. Dang. A hydro-mechanical modeling of double porosity and double permeability fractured reservoirs, PhD thesis, University of Orleans, France, 2018.